Published in final edited form as:
Nat Neurosci. 2004 October ; 7(10): 1059–1069. doi:10.1038/nn1317.

Control of axonal branching and synapse formation by focal adhesion kinase

Beatriz Rico[1], **Hilary E Beggs**, **Dorreyah Schahin-Reed**, **Nikole Kimes**, **Andrea Schmidt**, and **Louis F Reichardt**
Howard Hughes Medical Institute and Department of Physiology, University of California, San Francisco, California 94143, USA.

Abstract

The formation of neuronal networks in the central nervous system (CNS) requires precise control of axonal branch development and stabilization. Here we show that cell-specific ablation of the murine gene *Ptk2* (more commonly known as *fak*), encoding focal adhesion kinase (FAK), increases the number of axonal terminals and synapses formed by neurons *in vivo*. Consistent with this, *fak* mutant neurons also form greater numbers of axonal branches in culture because they have increased branch formation and reduced branch retraction. Expression of wild-type FAK, but not that of several FAK variants that prevent interactions with regulators of Rho family GTPases including the p190 Rho guanine nuclear exchange factor (p190RhoGEF), rescues the axonal arborization phenotype observed in *fak* mutant neurons. In addition, expression of a mutant p190RhoGEF that cannot associate with FAK results in a phenotype very similar to that of neurons lacking FAK. Thus, FAK functions as a negative regulator of axonal branching and synapse formation, and it seems to exert its actions, in part, through Rho family GTPases.

Control of axonal branch formation and retraction is necessary to establish the final pattern of connections between a neuron and its many cellular targets. Previous studies have shown that extracellular cues, such as neurotrophic factors, slits, ephrins, semaphorins, integrins and immunoglobulin family cell-adhesion molecules, regulate axonal branching, pruning and synapse formation[1–6]. These extracellular proteins act intracellularly, mainly through proteins that regulate assembly and disassembly of the cytoskeleton such as the Rho family of GTPases[7,8]. The pathways and molecules involved in the transfer of information from the environment to these more direct regulators of cytoskeleton dynamics are, however, not well understood.

A potential candidate to mediate the flow of information from the extracellular environment to the cytoskeleton and thereby to control axonal development is FAK, a nonreceptor protein tyrosine kinase that is expressed in almost all cells and is typically activated after the formation of integrin-dependent focal adhesions[9]. First, FAK expression is enriched in developing neuronal cell bodies and growth cones, suggesting that it might regulate the interactions between growing neurites and the extracellular matrix[10,11]. Second, several of the extracellular cues described above as regulators of axonal development have been shown to function upstream of FAK[12–14]. Third, FAK may act as an essential intracellular adaptor,

Correspondence should be addressed to L.F.R. (E-mail: lfr@cgl.ucsf.edu) and B.R. (E-mail: brico@umh.es).
[1]Present address: Instituto de Neurosciencias de Alicante, CSIC and Universidad Miguel Hernández, 03550 Sant Joan d'Alacant, Spain.

COMPETING INTERESTS STATEMENT
The authors declare that they have no competing financial interests.

because activation of FAK in response to integrin engagement leads to the formation of phosphotyrosine docking sites for several classes of signaling molecules[15]. Last, this kinase is a prominent constituent of focal adhesions—macromolecular complexes formed by the clustering of integrin receptors with intracellular proteins in fibroblasts and other types of cell[15]. In the developing nervous system, growth cones are highly motile and do not form genuine focal adhesions but show smaller adhesion point contacts similar to those found in highly motile cells[16]. Disassembly of these adhesion sites may occur when growing axons disengage from previously established contacts, a process that is likely to be required for their normal extension and retraction. Notably, FAK promotes the disassembly of focal adhesions in fibroblasts *in vitro*[17], suggesting that it may also regulate this process in neurons.

Analysis of the function of FAK during nervous system development is prevented by the early embryonic lethality of *fak* mutant mice[18]. To overcome this problem, we have used *fak* conditional mutant mice using Cre-*loxP*–mediated targeted recombination[19]. Because FAK has a role in controlling the initial stages of brain development, including basement membrane formation and neuronal migration[19,20], we have disrupted *fak* postnatally to study the role of FAK in axonal development and synapse formation. To this end, we have generated a *cre* line using the *L7* promoter, which is exclusively expressed in Purkinje cells at the time that they are collateralizing their axons and refining their synaptic connections in their main target, the deep cerebellar nuclei (DCN)[21,22]. Using this approach, we show that FAK regulates negatively the formation of axonal terminals and, as a consequence, synapse formation *in vivo*. Consistent with this, perturbation of FAK function *in vitro* through Cre-mediated deletion of the *fak* allele in Purkinje cells and hippocampal neurons, another type of neuron in which expression of FAK is enriched[10,11], results in the development of exuberant axonal arborizations. Visualization of growth dynamics in FAK-deficient axons also shows that FAK regulates axonal extension and enhances axonal pruning. Finally, we identify protein interactions sites on FAK that are required for normal development of axonal arbors.

Our results suggest that FAK mediates its function in controlling axonal dynamics, in part, by regulating the function of Rho family GTPases through the activation of p190RhoGEF. Taken together, our results suggest that FAK is an important regulator of axonal development, controlling the extension and pruning of axons and, consequently, synapse formation.

RESULTS

L7-mediated deletion and cerebellar architecture

To study *in vivo* the cell-autonomous role of FAK during axonal development, we generated a cell-specific *cre* line using the *L7* promoter (hereafter designated *L7cre*; Supplementary Fig. 1 online), which drives the postnatal expression of Cre exclusively in Purkinje cells of the cerebellum[23]. Analysis of the progeny of *Tg(L7cre)22LFR* mice crossed with *R26R* reporter mice showed that *L7cre*-mediated recombination is restricted to Purkinje cells in cerebellum (Fig. 1a–g).

FAK protein is expressed during cerebellar development and its expression continues until adulthood in Purkinje cells[10]. We found that *L7cre;fak^{flox};fak^{null}* mutant mice are born at normal ratios and survive into adulthood with subtle differences in motor coordination as compared with their control littermates (Supplementary Fig. 2 online). Despite the small contribution that Purkinje cells make to the mass of the cerebellum, western blot analysis showed that the amount of FAK tended to be lower in the cerebellum (22% ± 13, $n = 3$;

Note: Supplementary information is available on the Nature Neuroscience website.

Supplementary Fig. 1 online). Postnatal loss of FAK in Purkinje cells, however, did not affect the gross morphology of the cerebellum (Fig. 1h–o).

We next determined whether loss of FAK in Purkinje cells would have postsynaptic effects by affecting the development of synapses impinging on these cells. Morphological examination at the electron microscopy level and quantification of the number of granule cell to Purkinje cell synapses, which occur specifically on Purkinje cell spines, detected no significant differences between *fak* conditional mutant mice and controls (Fig. 1p–q and data not shown). These data are consistent with light microscopy observations indicating that the number of Purkinje cell spines is not affected in *fak* conditional mutant mice (data not shown).

Axonal terminals and synapses are increased in *fak* mutants

To determine whether FAK regulates the differentiation of axons and/or synapses formed by Purkinje cells, we first analyzed the distribution of GAD65 (an isoform of the γ-amino butyric acid (GABA) biosynthetic enzyme glutamic acid decarboxylase) in the main synaptic target of Purkinje cells, the DCN. These nuclei reach a mature synaptic pattern by postnatal day 10 (P10) to P12 (refs. 22). We found an increase of about 50% in the relative area labeled by GAD65 immunostaining in the DCN of *fak* conditional mutants mice as compared with littermate controls (100% control, 148.24 ± 7.72% mutant, $n = 4$, $P < 0.005$; Supplementary Fig. 3 online).

To investigate whether the increase in GAD65 immunoreactivity observed in *the fak* conditional mutants was due to a rise in the number of axonal terminals and synapses, we analyzed the ultrastructure of Purkinje cell–DCN synapses. Because the main input to the DCN arises from Purkinje cells, most synapses found in these nuclei are formed by Purkinje cell axons[21]. In agreement with the increase in GAD65 immunostaining, the density of synapses found in the DCN was significantly increased in *L7cre;fak^{flox};fak^{null}* mice (35% increment; 95.06 ± 6.87 control and 127.89 ± 2.60 mutant synapses per 1,000 μm^2, $n = 4$, $P < 0.01$; Fig. 2a–d).

The rise in the density of Purkinje cell–DCN synapses was largely due to a marked increase in the number of complex synapses found in *L7cre;fak^{flox};fak^{null}* mice, as compared with controls (107% increment; 18.27 ± 2.90 control and 37.9 ± 4.36 mutant synapses per 1,000 μm^2, $n = 4$, $P < 0.005$; Fig. 2a–d). In the hippocampus, these complex synapses, defined as having more than one synaptic density, have been described as perforated synapses[24], whereas in the cerebellum they have been observed regularly in the synaptic contacts formed by the axonal terminals of Purkinje cells onto dendrites or soma of DCN neurons[21]. The number of simple synapses (containing one synaptic density) was not significantly increased in *fak* conditional mutants as compared with controls (Fig. 2a–d and data not shown). Thus, loss of FAK results in a marked increase in the number of complex synapses formed by Purkinje cells.

We next addressed whether FAK-deficient synapses have additional morphological distinctions from control synapses by quantifying the number of docked and the reserve pool of vesicles at the synaptic density. Whereas no changes were detected in the reserve pool (data not shown), we detected a significant reduction in the number of vesicles docked per length of active zone in *fak* conditional mutants (30%; 12.51 ± 0.35 control and 9.05 ± 0.25 mutant vesicles per μm, $n = 4$, $P < 0.0005$; Fig. 2e–h). Thus, postnatal ablation of *fak* results in an increase in the number of synapses made by Purkinje cells, although their individual efficiency, as assessed by the number of docked vesicles, seems to be reduced (see also ref. [25]).

To determine whether this increase in complex synapses correlates with a rise in the number of axon terminals, we counted the number of terminals found in the DCN by electron microscopy. The total density of terminals containing synapses was 40% higher in mutants

than in controls (Fig. 2a–d,i). This rise was due to the marked increase in the number of terminals containing complex synapses in *fak* conditional mutants (137% increment; Fig. 2a–d,i); by contrast, a less prominent rise in the number of terminals containing simple synapses was detected. Notably, the number of synapses per terminal did not change in *fak* conditional mutants (Fig. 2j).

Purkinje cells are the primary GABAergic source of axonal terminals in the DCN[22]. To confirm that the terminals included in our quantification stem from Purkinje cell axons, we analyzed GAD65 expression by electron microscopy. Consistent with the above results, we found a 60% increase in the density of GAD65-immunoreactive terminals in the Purkinje cell–specific mutant (Fig. 2k–s). Thus, these results indicate that the increase in the number of synapses formed in the absence of FAK is probably secondary to the observed increase in the number of Purkinje cell axonal terminals.

Increased axonal arborization in *fak* mutant Purkinje cells *in vitro*

To understand the basis of the defects observed in the *fak* conditional mutant mice, we examined effects on axonal growth and branching resulting from the loss of FAK function *in vitro*. Cerebellar cultures from control and *fak* conditional mutant mice were plated independently and then stained at 14 d *in vitro* (DIV) with antibody to calbindin, which labels only Purkinje cells in the cerebellum. Because the polarity of the Purkinje cells is strongly evident, we identified the axons by their morphology. As compared with controls, we observed significant increases in the number of branchpoints or in the total length of the axonal arbor in Purkinje cells lacking FAK (Fig. 3a–g). The increase in the number of branchpoints was restricted to the higher order branches, which may reflect the fact that at P1, the time of culture establishment, significant *L7cre*-mediated recombination had not yet occurred *in vivo*.

The increase in the number of branches was not secondary to the elongation of the axonal arbor, because the ratio between the number of branches and the total axon length was also significantly higher in Purkinje cells lacking FAK than in controls (Fig. 3h). These observations are consistent with the *in vivo* observations described above and indicate that the mechanisms underlying the increases in Purkinje cell axonal terminals and synapses found in *fak* conditional mutant mice *in vivo* can be studied using neurons in culture.

FAK controls axonal arborization in hippocampal neurons *in vitro*

To determine whether FAK has a similar role in other neuronal populations, we cultured hippocampal cells from mice homozygous for the fak^{flox} allele and eliminated the *fak* gene *in vitro* by transfection with a *Cre* expression vector (*EGFP-Cre*, enhanced green flourescent protein fused to Cre). Hippocampal neurons are well characterized morphologically and developmentally, have elaborate axonal arbors, and express large amounts of FAK[10]. We transfected neurons at 3 DIV to interfere with the development, but not the initiation, of axons[26,27]. To allow for Cre-mediated recombination of the fak^{flox} allele and turnover of the FAK protein, we analyzed the cultures 3 d after transfection at 6 DIV. At this stage, most of the long neurites examined seemed to be axons because they expressed the dephosphorylated axon-specific form of the microtubule-associated protein tau, which is bound by the tau-specific monoclonal antibody (mAb) tau-1 (ref. 28 and Fig. 4a–g).

Deletion of *fak* induced a significant increase in the number of branchpoints and in the total length of the axonal arbor of hippocampal neurons (Fig. 4h–o and data not shown). As in Purkinje cells, the increase in the number of branches was not secondary to the elongation (Fig. 4p). The phenotypes described here were not due to any alteration caused by expression of Cre, because wild-type *cre*-transfected hippocampal neurons were identical to neurons transfected with pcDNA3 (Supplementary Fig. 4 online). We obtained similar results by

perturbing FAK in hippocampal neurons with an alternatively expressed carboxy-terminal fragment of FAK called FAK-related non-kinase (FRNK; Supplementary Fig. 5 online), which functions as a dominant-negative form of FAK[15].

Thus, interfering with FAK function *in vitro* in both cerebellar Purkinje cells and hippocampal neurons leads to the development of exuberant axonal branches, suggesting that FAK has a general role in controlling the axonal branching of CNS neurons.

Axonal dynamics in hippocampal cells after *fak* deletion *in vitro*

To determine whether FAK functions to inhibit the formation of new axonal branches or to promote the retraction and pruning of previously formed branches, we monitored branch dynamics between 6 and 7 DIV in identified hippocampal neurons cultured from mice homozygous for the *fak* allele after transfection with the *cre* expression plasmid. Cre-mediated recombination of *fak* in hippocampal neurons resulted in a prominent decrease in the number of branches that underwent spontaneous retraction between 6 and 7 DIV (50% reduction; Fig. 5a–g) and a clear increase in the number of new branches extended by the same neurons over the same period of time (137% increment; Fig. 5a–f,h). Thus, loss of FAK in hippocampal neurons reduces the probability of the retraction of existing axonal branches and increases the formation of new branches.

We next used time-lapse microscopy to examine the rate of growth cone advance in *cre*-transfected hippocampal neurons. Consistent with the time course experiments, we observed an increase in the number of axonal extensions and a reduction in the number of retractions in these neurons (data not shown). In addition, the number of immobile axons in the *cre*-transfected neurons was higher than in controls (data not shown). Unexpectedly, the average growth axonal speed of axons lacking FAK was decreased by about 65% as compared with controls (Figs. 5i–k, and Supplementary Videos 1 and 2 online). Thus, the absence of FAK in hippocampal neurons generates axons with abnormally low motility. These axons extend new branches that seldom retract.

Taken together, these results suggest FAK has a pivotal role in the cellular dynamics controlling the process of axonal branching and axonal growth in these neurons.

Control of axonal dynamics by FAK and Rho family GTPases

FAK signaling to the cytoskeleton is required to control axonal branching and growth cone advance. Small GTPases of the Rho subfamily, such as RhoA, are essential regulators of actin polymerization and myosin activity[29]. To identify possible molecular pathways leading to Rho activation through FAK-mediated signaling in hippocampal neurons, we examined the ability of wild-type FAK and various FAK mutants lacking individual protein interaction sites to restore the normal pattern of axonal growth after deletion of the endogenous *fak* gene by Cre. As a control, we simultaneously transfected neurons with plasmids expressing EGFP-Cre, DsRed and full-length FAK. A Myc tag epitope allowed us to monitor the expression of the latter plasmid and analysis was limited to those cells in which the three plasmids were expressed strongly. Expression of wild-type FAK completely rescued the axonal branching phenotype observed in neurons transfected with *cre* alone (Fig. 6a–c,g,h and Supplementary Table 1 online).

We thus expected to observe a similar phenomenon after the expression of FAK mutants, except for those in which the integrity of the mutated site was essential for regulating axonal branching. To determine whether FAK activation is required to regulate axonal branching, we used a variant containing a point mutation that disrupts an important autophosphorylation site of FAK (Myc-FAK^{Y397F}); this site is important for full activation of FAK and for the phosphorylation

of several other sites on FAK[15]. In addition, phosphorylated Tyr397 functions as a docking site for the recruitment of Src family kinases, phosphatidylinositol 3-kinase (PI3K) and phospholipase C-γ1 (PLC-γ1)[15]. Src mediates phosphorylation at other sites of FAK, creating additional Src homology domain 2 (SH2)-binding sites that are required for the transduction of signals to several downstream pathways[15]. Expression of Myc-FAK^{Y397F} rescued partially (~38%), but not completely, the exuberant axonal branching phenotype observed in *fak* mutant neurons, indicating that additional sites on FAK are also involved in regulating axonal branching (Fig. 6d,g–k and Supplementary Table 1 online).

RhoA activity is controlled through both exchange factors (RhoGEFs) and GTPase activators (RhoGAPs)[29]. Among them, GTPase regulator associated with FAK (Graf) and p190RhoGEF bind directly to FAK in neuronal cell lines (PC12 and Neuro-2a)[30,31]. p190RhoGEF is phosphorylated and activated by FAK[31], thereby increasing Rho activity in cells. Although Graf functions as a RhoGAP in nonneuronal cells, where it terminates Rho activity, overexpression studies suggest that it functions synergistically with Rho, possibly as a Rho effector, in PC12 cells and hence potentially in neurons[32]. In neuronal cells, therefore, interaction of FAK with either of these proteins seems likely to enhance the effectiveness of Rho, thereby inhibiting axonal branching.

To test this possibility, we attempted to rescue the phenotype observed in FAK-deficient (*cre*-transfected) neurons by expressing Myc-tagged FAK variants containing point mutations in regions crucial for interactions with each of these proteins. Transfection with a variant unable to bind Graf (Myc-FAK^{P878A})[30] did not rescue the branching phenotype completely in *fak* mutant neurons (Fig. 6e,g–i and Supplementary Table 1 online). A similar result was observed in *fak*-deficient neurons transfected with the Myc-FAK^{L1034S} variant (Fig. 6f–i and Supplementary Table 1 online), which is unable to bind either p190RhoGEF or the cytoskeletal adaptor paxillin[31,33,34]. These data are consistent with the possibility that FAK controls axonal behavior, in part, by promoting the activation or effectiveness of Rho.

Because association of paxillin with integrins has been shown to regulate the cytoskeleton through Rho family G proteins, thereby reducing lamellipodial stability and cell migration similar to effects of active Rho[35], it seemed important to obtain more direct evidence for the involvement of the neuronal GEF, p190RhoGEF, as an effector of FAK in neurons. We therefore overexpressed both control and mutant p190RhoGEF in hippocampal neurons. The mutant used, p190RhoGEF$^{\Delta 1292–1301}$, contains a truncation in a region known to be necessary for the interaction of p190RhoGEF and FAK[31]. We considered that if p190RhoGEF–FAK interactions mediate, at least in part, FAK function in axonal branching, then expression of p190RhoGEF$^{\Delta 1292–1301}$ might result in a phenotype similar to that observed in neurons lacking FAK (that is, excessive axonal arborization) through competition for Rho. Consistent with this expectation, mouse hippocampal neurons transfected with a plasmid expressing p190RhoGEF$^{\Delta 1292–1301}$ showed a significant increment in axonal arborization as compared with control neurons (cells transfected with pCDNA3 or wild-type p190RhoGEF; Fig. 7a,b,d,f–j).

To test whether the mutant p190RhoGEF affected the same pathway that is regulated by FAK activation, we overexpressed p190RhoGEF$^{\Delta 1292–1301}$ in a *fak* mutant background (Fig. 7e–j). We considered that if expression of the mutant p190RhoGEF disrupts a different signaling pathway controlling axonal arborization, then we would observe an additive effect on the axonal branching phenotype. The data indicated, however, that expression of this p190RhoGEF mutant did not further enhance axonal branching in neurons lacking FAK (compare Fig. 7c–f). Consequently, overexpression of the p190RhoGEF mutant seems to disrupt the same signaling pathway that is perturbed by the absence of FAK.

In summary, our results indicate that FAK controls axonal growth and branching in neurons and provide evidence that this occurs, in part, through the recruitment and activation of p190RhoGEF.

DISCUSSION

We have examined the role of FAK in axonal development *in vivo* by using mice that lack FAK specifically in Purkinje cells. As compared with controls, the Purkinje cells of *fak* conditional mutant mice formed significantly more axonal terminals and, consequently, more synapses on their targets—the neurons of the DCN. Absence of FAK similarly increased the number of axon branches in Purkinje cells cultured *in vitro*. We also found that the role of FAK in controlling axonal branching is not unique to Purkinje cells. Indeed, interfering with FAK function in hippocampal neurons by either Cre-mediated deletion of *fak* or by expression of FRNK, a dominant-negative form of FAK, resulted in an increase in axonal branching.

By imaging single axonal arbors, we have also shown that the exuberant axonal arborization found in these neurons is caused by both increased formation and reduced pruning of axonal branches, even though the growth cone of these axons advance at only a third of the rate of control neurons. Finally, we have found that FAK function in controlling axonal dynamics seems to be mediated, in part, through the recruitment of a Rho activator, p190RhoGEF, which in turn influences cytoskeletal behavior. Thus, FAK has a prominent role in controlling axonal dynamics of developing neurons through Rho-mediated signaling (Supplementary Fig. 6 online).

Increased axonal terminals and synapses in *fak* mutants

Postnatal ablation of FAK in Purkinje cells resulted in a significant increase in axonal terminals and consequently in synapses *in vivo.* In the DCN, the target of Purkinje cells, the total area of GABAergic terminals was increased by 50%. Consistent with this, we observed a 60% increase in the number of DCN terminals containing GAD65 immunoreactivity (expressed in Purkinje cell axons) by electron microscopy. In addition, the total density of terminals was increased by about 40% and the density of synapses was increased by 35%. Of note, the main contribution to the latter change came from the rise in the number of terminals containing complex synapses (synapses with more than one synaptic density), which showed an increase of 137%.

Because Purkinje cells are the only cells targeted in our *fak* conditional mutant, and complex synapses have been observed among the normal synapses that Purkinje cells form in the DCN[21], the increase in the number of terminals and complex synapses formed by *fak*-mutated Purkinje cells most probably reflects a rise in synaptic contacts made by these cells. Because the number of synapses per terminal does not significantly change in *fak* conditional mutants, the rise in the number of synapses observed in the DCN can be explained only by an increase in the number of axonal terminals made by Purkinje cells. Thus, light microscopic and electron microscopic analyses support the conclusion that more terminals are formed by Purkinje cells axons in the absence of FAK.

FAK as a negative regulator of axonal branch formation

The absence of FAK protein in neurons resulted in three main axonal phenotypes: reduced growth cone motility, increased probability of axonal branch extension, and reduced probability of axonal retraction or pruning. Time-lapse experiments showed that the rate of extension of axons lacking FAK was only a third of that of controls, and overexpression of FAK in hippocampal neurons has been shown to lead to a highly dynamic behavior of the growth cone[11]. Despite this, the final result is an increase in the total length of the axon arbors of Purkinje cells and hippocampal neurons, as well as an increase in the number of axonal

branchpoints. Both phenotypes (namely, reduced speed rate and increased total length) are not contradictory, because wild-type axons move forward and retract continuously, whereas FAK mutant axons hardly ever retract. Therefore, some mutant axons may extend for longer distances than some wild-type axons.

There is increasing evidence that many repulsive or attractive cues affect not only the behavior of the growth cone but also the initiation and extension of collateral branches from the axon shaft. For example, slit and glial cell-line derived neurotrophic factor (GDNF) have been shown to be involved in elongation as well as axonal branching[4,36]. Are the effects on growth cone motility and axonal branching related? In support of this possibility, growth cone pausing has been shown to be related to the formation of axonal branches *in vivo* and *in vitro*[37]. It remains possible, however, that FAK regulates these two processes by activating different signaling cascades.

Previous studies have shown that activation of FAK after costimulation of growth factor receptors and integrins promotes the outgrowth of neurites from PC12 and SH-SY5Y cells[38]. These results seem to be consistent with our finding that FAK is necessary to promote normal growth cone motility, although we also observed effects on axonal branch formation and stability that indicated that FAK activity reduces the total length of the axonal arbor formed by an individual neuron. The studies using PC12 and SH-SY5Y cells[38] primarily examined the effects of FAK on the initial extension of neurites from the cell body, whereas our studies examined the growth of axons from neurons that had initially expressed FAK. In PC12 and SH-SY5Y cells, association of paxillin with FAK seems to be necessary for normal neurite extension because overexpression of a paxillin mutant that cannot associate with FAK (an LD4 deletion mutant) inhibits neurite outgrowth[38]. Our experiments do not exclude the possibility that paxillin has a role in regulating axon growth or branch formation by hippocampal neurons. In view of data indicating that the association of paxillin with integrins actually inhibits cell motility in leukocytes[35], it will be interesting to determine whether paxillin promotes or inhibits growth cone motility in primary neurons.

Mediators of FAK interaction with the cytoskeleton

In addition to its function as a protein tyrosine kinase, FAK is a large adaptor protein with binding sites for many proteins involved in cell signaling and motility, including several growth factor receptors, integrins, PI3K, Src, p130CAS, RhoGTPases regulators (Graf, Trio, 190RhoGEF), the ArfGAP ASAP1 and cytoskeletal proteins such as paxillin[15,30,32,34]. Many of these proteins regulate activities of the Rho family of GTPases, which in turn control axon growth guidance and branching through regulation of the cytoskeleton[8]. Consistent with the possibility that FAK may function in neurons to promote branch retraction and to inhibit branch extension through RhoA, inhibition of RhoA has been shown to reduce neurite retraction and to increase branch extension, similar to phenotypes observed after loss of FAK[39,40]. Interactions between FAK and Rho are complex as they have been shown to regulate the activity of each other. On the one hand, Rho activation induces focal adhesion formation, thereby promoting FAK activation[41]. On the other hand, activation of FAK induces Rho downregulation, which reduces focal adhesions stability[42]. Loss of this regulatory loop is thought to explain the increase in focal adhesions and the reduced motility observed in *fak* mutant fibroblasts, and it may also explain the perturbations observed in *fak* mutant neurons.

Our data on the phenotype resulting from the expression of a FAK mutant that cannot recruit or activate p190RhoGEF in a *fak*-deficient background, together with the similarity in phenotype observed after deletion of *fak* or overexpression of a p190RhoGEF mutant that cannot associate with, provide evidence implicating FAK regulation of the Rho GTPase pathway in the control of axonal branching. The results indicate that p190RhoGEF is an effector of FAK through which FAK controls axonal arborization.

As Graf has been shown to be a RhoGAP in fibroblasts, it seems surprising that a mutation in FAK that disrupts its binding would have an effect similar to that of a mutation in the p190RhoGEF-binding site of FAK. Of note, even though Graf contains a GAP domain and has been shown to inactivate RhoA-GTP in fibroblasts[30], it synergizes with Rho in PC12 cells, suggesting that it is a celltype-specific Rho effector[30,32]. Our observations are most consistent with those made in PC12 cells and also suggest that Graf potentially functions as an effector of Rho signaling. It will be interesting to examine Graf function more directly using mutants and to characterize the pathway through which Graf synergizes with Rho in neurons. Alternatively, the P878A mutation in FAK might disrupt the binding of an unknown protein that is also important for controlling axonal branch formation.

Overexpression of RhoGAPs induces extensive outgrowth of long and highly branched neurites[7], raising the possibility that FAK can inhibit the activity of one or more proteins of the RhoGAP family. Although our results provide no direct evidence for this, they do show that a mutation in the recruitment site for Src kinase (FAK^{Y397F}) partially inhibits the ability of FAK to control axonal arborization. Src kinase, which is activated by FAK, has been shown to inhibit the activity of p190RhoGAP[8]. Expression of FAK^{Y397F} (containing a mutation in the Src recruitment site), FAK^{P878A} (a mutation in the Graf recruitment site) or FAK^{L1034S} (a mutation in the p190RhoGEF recruitment site) partially rescues the deficiency in axonal arbor formation observed in the complete absence of FAK in cultured hippocampal neurons (a decrease of 38%, 36% and 21%, respectively, in the total number of branches versus *cre*-transfected $fak^{flox};fak^{flox}$ neurons; Fig. 6g and Supplementary Table 1 online). This suggests that FAK may control axonal branching dynamics by coordinating activation of a RhoGEF (p190RhoGEF), recruitment of a Rho effector (Graf or another protein) and inhibition of a RhoGAP (possibly p190RhoGAP).

FAK, extracellular signaling molecules and neuronal plasticity

Several diffusible factors, among them neurotrophins and slits, membrane-bound ligands such as ephrins, and adhesion-promoting receptors including integrins, have been shown to regulate axonal branching and synaptogenesis[1–5]. For example, ephrins and semaphorins mediate axonal branch pruning and spine retraction in hippocampal neurons[6,43,44]. FAK is activated by ephrins and Eph receptors[12,14], suggesting that it may directly mediate some of the functions of these and other guidance cues, especially those known to be involved in regulating axonal branching, such as slits and semaphorins[4,6].

Although our studies have shown that FAK affects the formation of axonal arbors during development, it seems possible that the presence of FAK in the mature nervous system may be required to permit neurons to reorganize their axonal arbors and synapses in the synaptic reorganization that accompanies learning[45]. Accordingly, FAK seems to be required for the induction of long-term potentiation in dentate gyrus[46]. In future studies, it will be interesting to determine whether FAK regulates the long-term plastic changes that occur in the adult brain and whether these changes involve the same signaling pathways that are important during neuronal development.

METHODS

Transgenic mouse strains

Mice lacking FAK in Purkinje cells were produced by breeding mice carrying a *loxP*-flanked *fak* allele with transgenic mice in which the *L7* promoter drives expression of Cre recombinase (Supplementary Fig. 1a online). Mouse procedures were approved by the University of California San Francisco Committee on Animal Research.

Electron microscopy

Mice were perfused and postfixed as described[47] for conventional electron microscopy (CEM). For immunoelectron microscopy (IEM), mice were perfused as for CEM and the brains were removed and post-fixed for 2 h in the same fixative. For both techniques, brains were sectioned by vibratome (at 200 μm for CEM and 100 μm for IEM), and the most medial slices selected. For CEM, slices were postfixed for 1 h in 2% osmium tetroxide and 0.1 M sodium cacodylate (pH 7.4), dehydrated in a series of ethanol dilutions, and embedded flat in an Epon-Araldite mixture. For IEM, free-floating sections were incubated with mouse antibody to GAD65 as described for light microscopy immunohistochemistry, and then stained with osmium tetroxide and processed as for CEM.

We used semithin sections stained with toluidine blue to identify and to trim the medial sagittal plane of the fastigial nucleus, the most medial DCN. Ultrathin sections were cut and stained with uranyl acetate and lead citrate for CEM. The sections were not stained for IEM. Quantitative analyses were done blind to genotype. We took 15–20 electron micrographs from the DCN at a final magnification of ×35,000 for each genotype in each experiment ($n = 4$). Total numbers of synapses, simple synapses and complex synapses were quantified per 1,000 μm^2. We counted only synapses containing well-identified active zones and vesicles. The same electron micrographs were used to quantify the axonal terminals. Only terminals containing the previously defined simple or complex synapses were computed. In general, most of the terminals contained either one simple or one complex synapse, but a few contained both simple and complex synapses. Terminals containing dark inclusions were counted for the IEM experiments (20 micrographs of $n = 3$ mice for each genotype were selected).

Divergence in the increment in number of terminals between both quantifications (CEM and IEM) could be explained by the different counting criteria used. Indeed, whereas in the first quantification we counted just the terminals containing synapses, in the second one, owing to the dark precipitates of diamino-benzine (DAB), we computed all terminals, which might or not contain synapses. We counted the docked and reserved vesicle pools according to described criteria[48] ($n = 4$, 800 synapses analyzed). In brief, the number of docked vesicles per micrometer of each individual active zone was quantified and then averaged, so that the reduction in docked vesicles was independent of the increase in total active zone length.

Culture experiments and image acquisition

Cerebella from control mice and *fak* conditional mutants (*L7cre;fak*^{flox}*;fak*^{null} and *L7cre;fak*^{flox}*;fak*^{flox}) at P1 were prepared as described[49]. Cells were plated on 20-mm diameter Delta T dishes (Bioptechs) coated with poly-L-lysine (0.5 mg/ml in 100 mM borate buffer, pH 8.5; Sigma). The cultures were maintained until 14 DIV, fixed with 4% paraformaldehyde in 5% glucose PBS and immunostained overnight with rabbit antibody to calbindin (diluted 1:5,000; Swant).

Rat hippocampi from fetal rats at embryonic day 18 (E18) or from *fak*^{flox}*;fak-*^{flox} mice at P0 were dissected, treated with trypsin (0.25% for 20 min at 37 °C) and dissociated by trituration as described[50]. Cells were plated on 20-mm diameter Delta T dishes coated with poly-L-lysine in MEM containing 10% horse serum, 1 mM pyruvate, penicillin-streptomycin and 0.6% glucose (‘plating medium’). Neurons were plated at densities of 150 and 200 cells per mm^2 for rats and mice, respectively. After 4 h, the plating medium was replaced by Neurobasal media, penicillin-streptomycin and B27 supplements (‘maintenance medium’). Neurons were transfected using Effectene (Qiagen) in accordance with the kit instructions. The transfection efficiency was about 1% (ref. 50).

All cultures were cotransfected with plasmids containing EGFP or DsRed reporters to visualize the morphology of the transfected neuron. For rat hippocampal cultures, plasmids expressing dominant-negative FRNK (pCDNA3-FRNK; a gift of T. Parsons, University of Virginia, VI) or control plasmids (pCDNA3) were cotransfected (2:1) with plasmids expressing EGFP (pCS2-EGFP; Clontech) or DsRed (pDsRed2-N1; Clontech) at 4 DIV. For murine hippocampal cultures, plasmids expressing Cre-EGFP (pBS505; a gift of B. Sauer, Oklahoma Medical Research Foundation, OK) or control plasmids were cotransfected with the plasmids EGFP or DsRed plasmids at 3 DIV. Controls experiments to ensure the naive expression of Cre were carried out in a wild-type background (CD1). The efficiency of the Cre-expressing plasmid has been shown using the reporter *R26R* and other floxed alleles[50].

For the triple transfections, we improved the survival of the cultures by using hippocampi from E18 fetal mouse. Note that the values for both branch number and axon length per neuron are augmented in Figures 6 and 7. Because each experiment has its own independent controls, these differences do not affect the results. The Myc-FAKwt, Myc-FAK^{Y397F}, Myc-FAK^{P878A} and Myc-FAK^{L1034S} point mutation constructs, a gift of J.T. Parsons (University of Virginia, VA), were coexpressed with the Cre-EGFP and DsRed plasmids in *fak*^{flox}/*fak*^{flox} hippocampal neurons (2:2:1). The pCDNA-p190RhoGEFfull-length construct, a gift of W.H. Moolenaar (The Netherlands Cancer Institute, Netherlands), was cotransfected with the DsRed plasmid (2:1). To generate the p190RhoGEF deletion mutant, two polymerase chain reaction (PCR) segments, spanning residues 1,023–1,347 in full-length p190RhoGEF, were generated. These segments did not contain residues 1,292–1,301 (DVSQSSEESP), which have been shown to promote FAK association[31]. The truncated isoform, Cre-EGFP and DsRed plasmids were triply transfected into *fak*^{flox}/*fak*^{flox} or wild-type hippocampal neurons (2:2:1).

Image processing and analysis

Random transfected neurons were imaged using a Zeiss Axiovert 200M deconvolution microscope (10×/0.5 Plan Apochromat) modified for SlideBook (3.0.10.5; Intelligent Imaging Innovations) or a Zeiss inverted LSM 5 Pascal confocal microscope (10×/0.30 and 20×/0.5 Plan Neofluar). All images were captured under the same conditions within each type of experiment. After conversion to TIFF format, the selected images were exported to Image J (National Institutes of Health (NIH) software) for drawing neuronal arbors and final quantification. The obvious polarity of the Purkinje cells allowed us to identify Purkinje cell axons by morphology.

For hippocampal neurons, to estimate which percentage of axonal branches were represented in our neurite population at the stages studied, we used immunohistochemistry with antibodies to the axon-specific form of tau. Random fields were selected from two independent experiments. We quantified 155 neurite branches from ten neurons labeled with DsRed. Taupositive collaterals were counted as axonal branches. Several morphological parameters were analyzed. Neurites longer than 15 μm were traced and counted as branches. Branch order criteria were chosen by following the distance in branches from the first branchpoint. Total neurite length was determined by summing the lengths of all neurites for each neuron. The same neuron was recorded at 6 DIV and 24 h later for the time course experiments to study axonal dynamics. Gain of neurites in the neuron recorded at 7 DIV was quantified as extension. Loss of neurites at 7 DIV in comparison to 6 DIV was counted as retraction. Neurites that changed their length were not included in the quantification.

For the time-lapse experiments, axons from neurons transfected with pcDNA3 or the Cre plasmid were recorded over 3 h. To ensure that the neurites were axons and not dendrites, we carefully selected endings of axons located at a distance of roughly more than 1,000 μm from the cell body. In cultures at 6 DIV, tau-negative processes were hardly ever observed at a distance of more than 400 μm from the soma. The axonal speed rate was calculated by

subtracting the initial length to the final length of each particular axon (the axonal forward and backward advance) in micrometers per second of recording. Overall significant differences between conditions were determined by the *t*-test for pair comparisons, and by one-way analysis of variance (ANOVA) for multiple comparisons. Post-hoc comparisons were done with Fisher's PLSD test.

ACKNOWLEDGMENTS

We thank D. Ilic and P. Soriano for the *fak*^{null} and *R26R* strains; J. Oberdick for the *L7* minigen; G. Martin for the Cre plasmid; B. Sauer for the Cre-EGFP plasmid; T. Parsons for the FRNK, Myc-FAKwt, Myc-FAK^{Y397F}, Myc-FAK^{P878A} and Myc-FAK^{L1034S} constructs; W.H. Moolenaar for p190RhoGEF; O. Marín, S. Bamji, M. Stryker and C. Damsky for comments on the manuscript; members of L.F.R.'s laboratory for discussions; C. Mason, H. Heuer and S. Bamji for advice on cultures; S. Huling for assistance with electron microscopy; and O. Marín and S. Martínez for infrastructure support. This work was supported by a grant from the NIH and by the Howard Hughes Medical Institute (HHMI). B.R. was supported by a grant from the Ministerio de Educación y Cultura of Spain and by the HHMI. L.F.R. is an Investigator of the HHMI. B.R. is a Ramón y Cajal Investigator from Ministerio de Ciencia y Tecnología of Spain.

References

1. Frisen J, et al. Ephrin-A5 (AL-1/RAGS) is essential for proper retinal axon guidance and topographic mapping in the mammalian visual system. Neuron 1998;20:235–243. [PubMed: 9491985]
2. Seki T, Rutishauser U. Removal of polysialic acid-neural cell adhesion molecule induces aberrant mossy fiber innervation and ectopic synaptogenesis in the hippocampus. J. Neurosci 1998;18:3757–3766. [PubMed: 9570806]
3. Vicario-Abejón C, Collin C, McKay RD, Segal M. Neurotrophins induce formation of functional excitatory and inhibitory synapses between cultured hippocampal neurons. J. Neurosci 1998;18:7256–7271. [PubMed: 9736647]
4. Wang KH, et al. Biochemical purification of a mammalian Slit protein as a positive regulator of sensory axon elongation and branching. Cell 1999;96:771–784. [PubMed: 10102266]
5. Rohrbough J, Grotewiel MS, Davis RL, Broadie K. Integrin-mediated regulation of synaptic morphology, transmission, and plasticity. J. Neurosci 2000;20:6868–6878. [PubMed: 10995831]
6. Bagri A, Cheng HJ, Yaron A, Pleasure SJ, Tessier-Lavigne M. Stereotyped pruning of long hippocampal axon branches triggered by retraction inducers of the semaphorin family. Cell 2003;113:285–299. [PubMed: 12732138]
7. Brouns MR, Matheson SF, Settleman J. p190 RhoGAP is the principal Src substrate in brain and regulates axon outgrowth, guidance and fasciculation. Nat. Cell Biol 2001;3:361–367. [PubMed: 11283609]
8. Billuart P, Winter CG, Maresh A, Zhao X, Luo L. Regulating axon branch stability: the role of p190 RhoGAP in repressing a retraction signaling pathway. Cell 2001;107:195–207. [PubMed: 11672527]
9. Schaller MD, et al. pp125FAK a structurally distinctive protein-tyrosine kinase associated with focal adhesions. Proc. Natl. Acad. Sci. USA 1992;89:5192–5196. [PubMed: 1594631]
10. Menegon A, et al. FAK^{+} and PYK2/CAKβ, two related tyrosine kinases highly expressed in the central nervous system: similarities and differences in the expression pattern. Eur. J. Neurosci 1999;11:3777–3788. [PubMed: 10583467]
11. Contestabile A, Bonanomi D, Burgaya F, Girault JA, Valtorta F. Localization of focal adhesion kinase isoforms in cells of the central nervous system. Int. J. Dev. Neurosci 2003;21:83–93. [PubMed: 12615084]
12. Cowan CA, Henkemeyer M. The SH2/SH3 adaptor Grb4 transduces B-ephrin reverse signals. Nature 2001;413:174–179. [PubMed: 11557983]
13. Beggs HE, Baragona SC, Hemperly JJ, Maness PF. NCAM140 interacts with the focal adhesion kinase p125^{fak} and the SRC-related tyrosine kinase p59^{fyn}. J. Cell Biol 1997;272:8310–8319.
14. Miao H, Burnett E, Kinch M, Simon E, Wang B. Activation of EphA2 kinase suppresses integrin function and causes focal-adhesion-kinase dephosphorylation. Nat. Cell Biol 2000;2:62–69. [PubMed: 10655584]

15. Parsons JT. Focal adhesion kinase: the first ten years. J. Cell Sci 2003;116:1409–1416. [PubMed: 12640026]
16. Arregui CO, Carbonetto S, McKerracher L. Characterization of neural cell adhesion sites: point contacts are the sites of interaction between integrins and the cytoskeleton in PC12 cells. J. Neurosci 1994;14:6967–6977. [PubMed: 7965092]
17. Webb DJ, Parsons JT, Horwitz AF. Adhesion assembly, disassembly and turnover in migrating cells —over and over and over again. Nat. Cell Biol 2002;4:E97–E100. [PubMed: 11944043]
18. Ilic D, et al. Reduced cell motility and enhanced focal adhesion contact formation in cells from FAK-deficient mice. Nature 1995;377:539–544. [PubMed: 7566154]
19. Beggs HE, et al. FAK deficiency in cells contributing to the basement membrane results in cortical abnormalities resembling congenital muscular dystrophies. Neuron 2003;40:501–514. [PubMed: 14642275]
20. Xie Z, Sanada K, Samuels BA, Shih H, Tsai LH. Serine 732 phosphorylation of FAK by Cdk5 is important for microtubule organization, nuclear movement, and neuronal migration. Cell 2003;114:469–482. [PubMed: 12941275]
21. Chan-Palay, V. Cerebellar Dentate Nucleus. New York: Springer; 1977.
22. Garin N, Hornung JP, Escher G. Distribution of postsynaptic $GABA_A$ receptor aggregates in the deep cerebellar nuclei of normal and mutant mice. J. Comp. Neurol 2002;447:210–217. [PubMed: 11984816]
23. Oberdick J, Levinthal F, Levinthal C. A Purkinje cell differentiation marker shows a partial DNA sequence homology to the cellular sis/PDGF2 gene. Neuron 1988;1:367–376. [PubMed: 2483097]
24. Sorra KE, Fiala JC, Harris KM. Critical assessment of the involvement of perforations, spinules, and spine branching in hippocampal synapse formation. J. Comp. Neurol 1998;398:225–240. [PubMed: 9700568]
25. Davis GW, Bezprozvanny I. Maintaining the stability of neural function: a home-ostatic hypothesis. Annu. Rev. Neurosci 2001;63:847–869.
26. Bradke F, Dotti CG. Differentiated neurons retain the capacity to generate axons from dendrites. Curr. Biol 2000;10:1467–1470. [PubMed: 11102812]
27. Mantych KB, Ferreira A. Agrin differentially regulates the rates of axonal and dendritic elongation in cultured hippocampal neurons. J. Neurosci 2001;21:6802–6809. [PubMed: 11517268]
28. Mandell JW, Banker GA. A spatial gradient of tau protein phosphorylation in nascent axons. J. Neurosci 1996;16:5727–5740. [PubMed: 8795628]
29. Luo L. Actin cytoskeleton regulation in neuronal morphogenesis and structural plasticity. Annu. Rev. Cell Dev. Biol 2002;18:601–635. [PubMed: 12142283]
30. Hildebrand JD, Taylor JM, Parsons JT. An SH3 domain containing GTPase-activating protein for Rho and cdc42 associates with focal adhesion kinase. Mol. Cell. Biol 1996;16:3169–3178. [PubMed: 8649427]
31. Zhai J, et al. Direct interaction of focal adhesion kinase with p190RhoGEF. J. Biol. Chem 2003;278:24865–24873. [PubMed: 12702722]
32. Taylor JM, Macklem MM, Parsons JT. Cytoskeletal changes induced by GRAF, the GTPase regulator associated with focal adhesion kinase,are mediated by Rho. J. Cell Sci 1999;112:231–242. [PubMed: 9858476]
33. van Horck FP, Ahmadian MR, Haeusler LC, Moolenaar WH, Kranenburg O. Characterization of p190RhoGEF, a RhoA-specific guanine nucleotide exchange factor that interacts with microtubules. J. Biol. Chem 2001;276:4948–4956. [PubMed: 11058585]
34. Klingbeil CK, et al. Ta rgeting Pyk2 to β1-integrin-containing focal contacts rescues fibronectin-stimulated signaling and haptotactic motility defects of focal adhesion kinase-null cells. J. Cell Biol 2001;152:97–110. [PubMed: 11149924]
35. Goldfinger LE, Han J, Kiosses WB, Howe AK, Ginsberg MH. Spatial restriction of α4 integrin phosphorylation regulates lamellipodial stability and α4β1-dependent cell migration. J. Cell Biol 2003;162:731–741. [PubMed: 12913113]
36. Markus A, Patel TD, Snider WD. Neurotrophic factors and axonal growth. Curr. Opin. Neurobiol 2002;12:523–531. [PubMed: 12367631]

37. Kalil K, Szebenyi G, Dent EW. Common mechanisms underlying growth cone guidance and axon branching. J. Neurobiol 2000;44:145–158. [PubMed: 10934318]
38. Ivankovic-Dikic I, Grönroos E, Blaukat A, Barth B-U, Dikic I. Pyk2 and FAK regulate neurite outgrowth induced by growth factors and integrins. Nat. Cell Biol 2000;2:574–581. [PubMed: 10980697]
39. Li Z, Van Aelst L, Cline HT. Rho GTPases regulate distinct aspects of dendritic arbor growth in *Xenopus* central neurons *in vivo*. Nat. Neurosci 2000;3:217–225. [PubMed: 10700252]
40. Thies E, Davenport RW. Independent roles of Rho-GTPases in growth cone and axonal behavior. J. Neurobiol 2002;54:358–369. [PubMed: 12500311]
41. Barry ST, Flinn HM, Humphries MJ, Critchley DR, Ridley AJ. Requirement for Rho in integrin signaling. Cell Adhes. Commun 1997;4:387–398. [PubMed: 9177901]
42. Ren XD, et al. Focal adhesion kinase suppresses Rho activity to promote focal adhesion turnover. J. Cell Sci 2000;113:3673–3678. [PubMed: 11017882]
43. Gao P-P, Yue Y, Cerretti DP, Dreyfus C, Zhou R. Ephrin-dependent growth and pruning of hippocampal axons. Proc. Natl. Acad. Sci. USA 1999;96:4073–4077. [PubMed: 10097165]
44. Murai KK, Nguyen LN, Irie F, Yamaguchi Y, Pascuale EB. Control of hippocampal dendritic spine morphology through ephrin-A3/EphA4 signalling. Nat. Neurosci 2003;6:153–160. [PubMed: 12496762]
45. Yuste R, Bonhoeffer T. Morphological changes in dendritic spines associated with long-term synaptic plasticity. Annu. Rev. Neurosci 2001;24:1071–1089. [PubMed: 11520928]
46. Yang YC, Ma YL, Chen SK, Wang CW, Lee EH. Focal adhesion kinase is required, but not sufficient, for the induction of long-term potentiation in dentate gyrus neurons *in vivo*. J. Neurosci 2003;23:4072–4080. [PubMed: 12764094]
47. Rico B, Xu B, Reichardt LF. TrkB receptor signaling is required for establishment of GABAergic synapses in the cerebellum. Nat. Neurosci 2002;5:225–233. [PubMed: 11836532]
48. Pozzo-Miller LD, et al. Impairments in high-frequency transmission, synaptic vesicle docking, and synaptic protein distribution in the hippocampus of BDNF knockout mice. J. Neurosci 1999;19:4972–4983. [PubMed: 10366630]
49. Baptista CA, Hatten M, Blazeski R, Mason CA. Cell-Cell interactions influence survival and differentiation of purified purkinje cells *in vitro*. Neuron 1994;12:243–260. [PubMed: 8110456]
50. Bamji SX, et al. Role of β-catenin in synaptic vesicle localization and presynaptic assembly. Neuron 2003;40:719–731. [PubMed: 14622577]

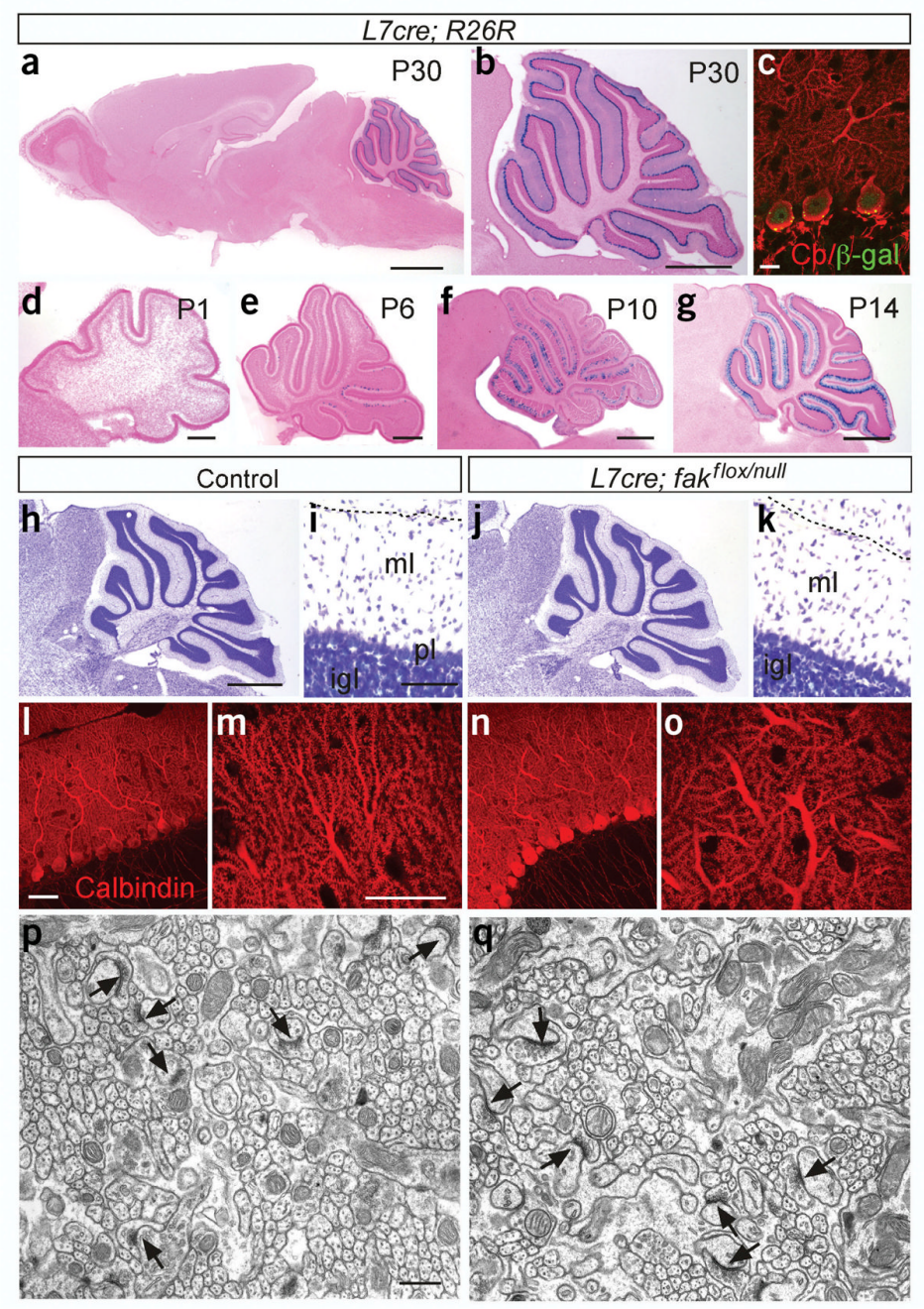

Figure 1.

L7-driven Cre-mediated deletion of the *R26R* and *fak* alleles and cerebellar architecture in *fak* conditional mutant mice at P30–P40. (**a–g**) Spatiotemporal development of *L7cre*-mediated recombination in the *R26R* mice, identified by expression of the reporter *lacZ*. (**a**) Saggital view of an adult brain showing expression of *lacZ* at P30. Recombination was nearly complete in cerebellar Purkinje cell with almost no recombination elsewhere. A few scattered cells were detected in the cortex. No expression was detected in other CNS or peripheral nervous system regions (not shown). (**b**) Higher magnification of the cerebellar region of **a**. (**c**) Single confocal plane images illustrate colocalization of β-galactosidase (green puncta) and calbindin (red), a Purkinje cell marker. (**g**) Scattered Purkinje cells expressing *lacZ* were detected in the posterior

cerebellar lobules before P6. (**e**) Low levels of recombination were observed in the posterior lobules at P6. Only a few recombined cells are present in the anterior lobules. (**f**) At P10, high recombination was observed in Purkinje cells in all lobules except VI, VII and X. (**g**) Adult levels of recombination in Purkinje cells were reached by P14, except in lobules VI and VII, where many neurons were still not recombined. (**h–q**) Cerebellar architecture in P30–P40 *fak* conditional mutant mice. (**h–k**) Nissl-stained sagittal sections of control(**h,i**) and *L7cre;fak*^{flox}*;fak*^{null} mutant (**j, k**) mice. (**i,k**) Higher magnification images from lobule IV. There were no obvious differences in cerebellar folia development, laminar organization or cross-sectional areas of the molecular and granule cell layers between control and mutant mice. FAK controls the *in vitro* survival of different types of cell including fibroblasts and tumoral cells[15]. No significant changes in the density or organization of Purkinje cells was observed, suggesting that FAK is not required for survival of these neurons *in vivo*. (**l–o**) Calbindin staining showing the dendritic tree of the Purkinje cells and the spines at higher magnification. Although the complexity of dendritic arbors was not examined in detail, calbindin staining showed that the primary dendrites, secondary dendrites and spines of Purkinje cells were present and normally differentiated in conditional mutant mice. (**p,q**) Granule cell to Purkinje cell synapses at electron microscopy. These synapses are normal in morphology and number ($n = 3$, $P < 0.58$). FAK has been shown to transduce survival signals from the extracellular matrix in fibroblasts and tumor cells[15]; in contrast, our results show that FAK is not required for neuronal survival during development. Scale bars, 500 μm (**a,b,j**); 100 μm (**i**,**k**); 50 μm (**b,d–g**); 20 μm (**l–o**); 15 μm (**c**); 0.5 μm (**p,q**).

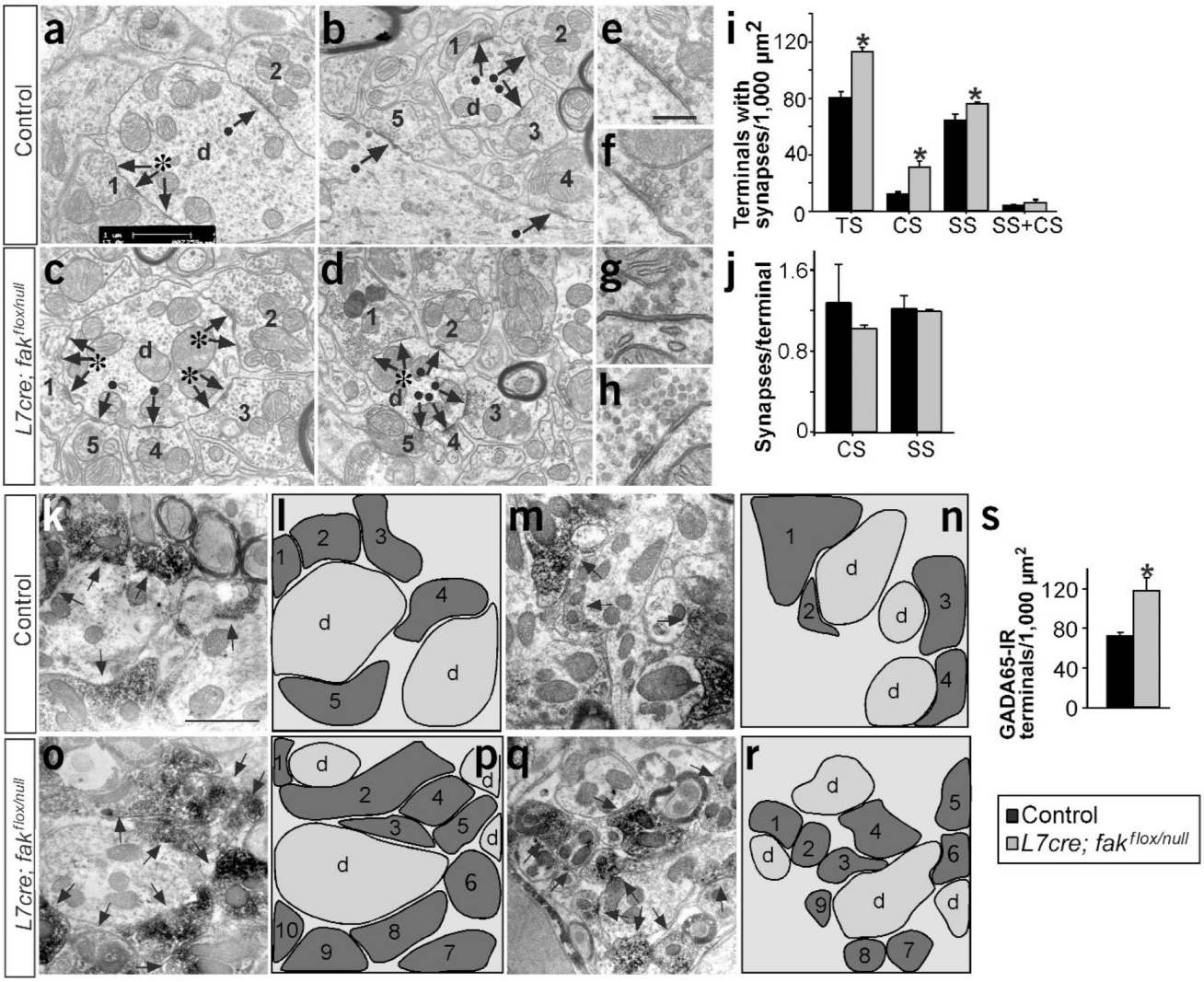

Figure 2.

Numbers of Purkinje cell axon terminals and synapses are increased in the DCN of *L7cre;fak*^{flox}*;fak*^{null} conditional mutant mice. (**a–d**) Fine structure of several representative fields in the DCN, showing terminals arriving and making synapses on the dendrite. Arrows indicate synaptic densities. Black dots indicate simple (1 synaptic density) and asterisks indicate complex (>1 synaptic density) synapses. Numbers identify the axonal terminals. d, dendrite. (**e–h**) Higher magnifica-tion images showing organization of the vesicles in the synaptic densities in the DCN. (**i**) Quantification of the number of terminals per 1,000 µm^2 containing different types of synapse (CS, complex; SS, simple; TS, total). *$P < 0.01$ to $P < 0.001$ versus control by ANOVA (control, 80.06 ± 4.24 TS, 12.25 ± 1.19 CS, 64.01 ± 4.40 SS; mutant, 112.57 ± 2.95 TS, 30.97 ± 4.84 CS, 75.60 ± 4.77 SS; $n = 4$). (**j**) Quantification of complex and simple synapses per terminal. (**k–r**) Electron micrographs showing representative fields, and schematic drawings of GAD65-immunoreactive (IR) axonal terminals in the DCN. Arrows indicate GAD65-IR axonal terminals. (**s**) Quantification of GAD65-IR terminals. *$P < 0.05$ versus control (control, 71.66 ± 3.58, $n = 3$; mutant, 117.61 ± 12.98, $n = 4$). Data are the mean ± s.e.m. Scale bars, 1 µm (**a–b**,**k–r**); 0.5 µm (**e–h**).

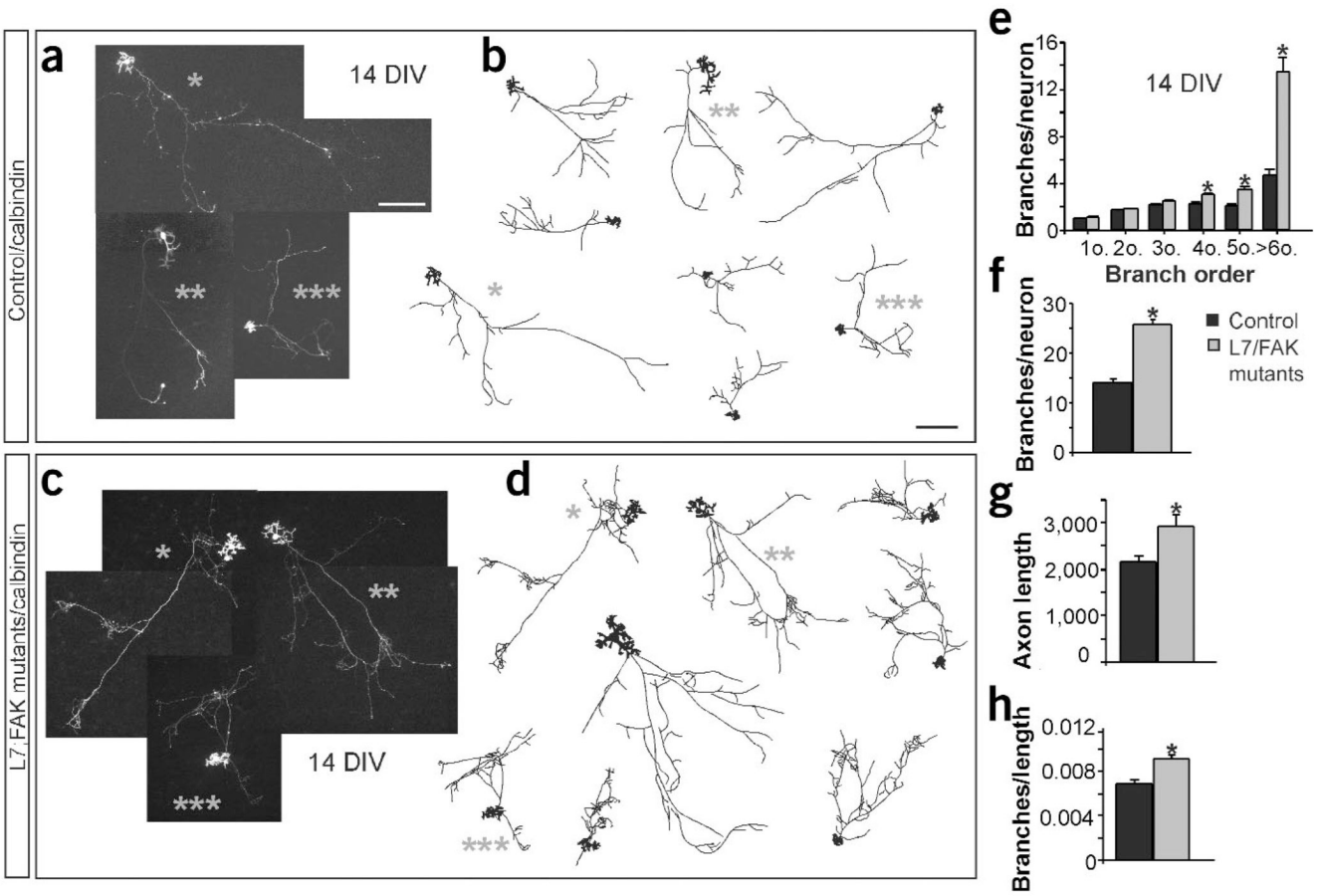

Figure 3.

Numbers of branches in Purkinje cells are increased in the absence of FAK *in vitro*. (**a–h**) Cerebellar mixed cultures from control and *L7Cre;fak* conditional mutant mice conditional mutant mice. (**a–d**) Fluorescence images and representative drawings of neurons from control (**a,b**) or mutant (**c,d**) mice at 14 DIV. Gray asterisks identify the drawing of the neurons shown in the adjacent photomicrographs.(**e**) Quantification of increasing branch orderper neuron. **P* < 0.0005 to *P* < 0.0001 versus control by two-tailed *t*-test (*n* = 115 neurons from three control and six conditional mutant cultures in **e–h**). (**f**) Quantification of the branches per neuron. **P* < 0.0001 versus control (control, 14.03 ± 0.59; mutant, 25.5 ± 1.12).**g**) Quantification of the total axon length per neuron expressed in µm. **P* < 0.0001 versus control (control, 2,163.9 ± 144.93;mutant,2,941.822 ± 231.06). (**h**) Quantification of the total number of branches per µm of axon. **P* < 0.0001 versus control (control, 0.0069 ± 0.0.00028; mutant, 0.0092 ± 0.00035). Data are the mean ± s.e.m. Scale bar, 200 µm (**a–d**).

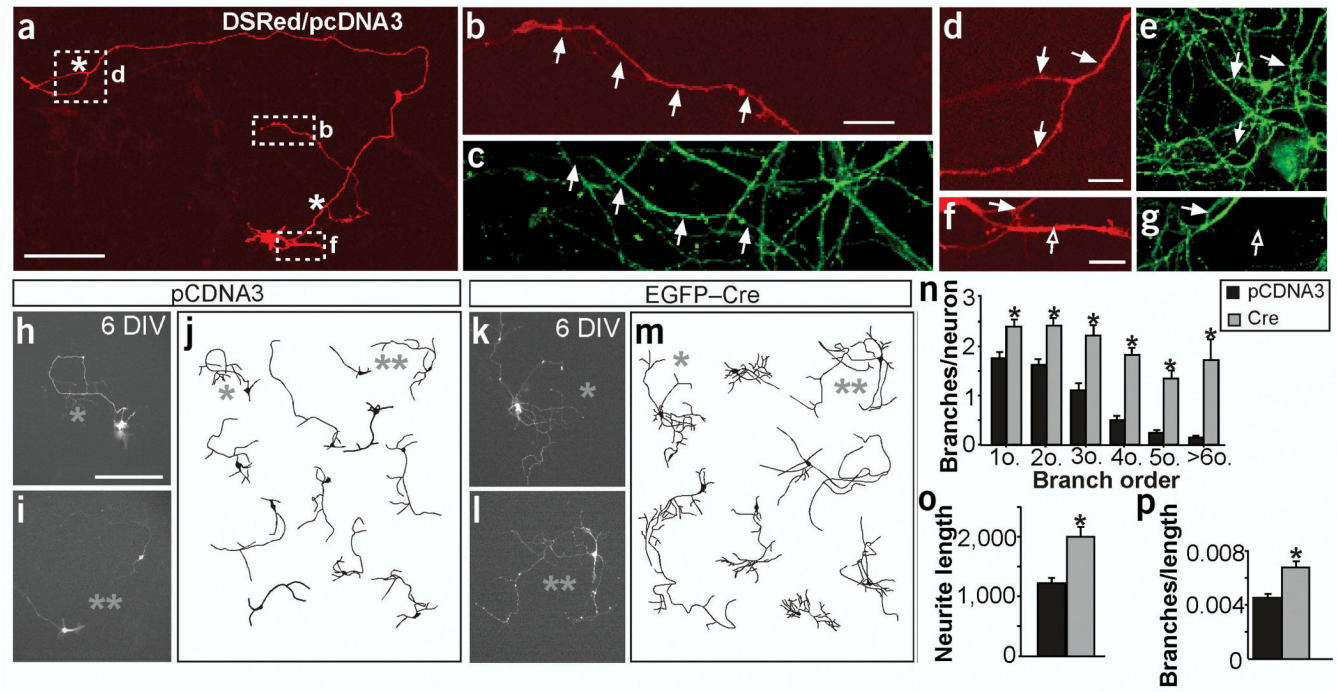

Figure 4.

DsRed and tau-1 are colocalized and branch numbers are increased in hippocampal cells in the absence of FAK at 6 DIV *in vitro*. At early stages, most of the neurites in these cultures express tau-1 in neurons transfected with control (shown here) and Cre- or FRNK-expressing plasmids (not shown). (**a,b,d,f**) Expression of DsRed and pCDNA. (**c,e,g**) Tau-1 immunoreactivity. (**b,d,f**) Higher magnification images corresponding to the boxed regions indicated in **a**. Most branching neurites at these stages are developing axons as they express the axon-specific marker tau-1 (~95%, $n = 10$ neurons). Arrows help to position the colocalization. Filled arrows indicate axons (tau-positive neurites), open arrows indicate dendrites (tau-negative neurites), white asterisks indicate branchpoints. (**h–p**) fak^{flox} deletion in mouse hippocampal cultures. (**h–m**) Fluorescence images and representative drawings of neurons transfected with control pCDNA3 (**h–j**) or Cre plasmid (**k–m**) at 6 DIV. (**n**) Quantification of branches at increasing branch orders per neuron. *$P < 0.01$ to $P < 0.0001$ versus control by two-tailed t-test ($n = 92$ neurons from four cultures in **n–p**). (**o**) Quantification of the total neurite length per neuron expressed in μm.*$P < 0.0005$ versus control (control 1,241.36 ± 93.24, mutant 2,018.04 ± 169.44). (**p**) Quantification of the total branches per μm of axon. *$P < 0.0005$ versus control (control 0.0045 ± 0.0003, mutant 0.0067 ± 0.0005). Note that, as described above, most branching neurites at these stages are developing axons (~95%), although a few of them could be dendrites. Data are the mean ± s.e.m. Scale bars, 200 μm (**n**,**m**); 100 μm (**a**); 10 μm (**b–g**).

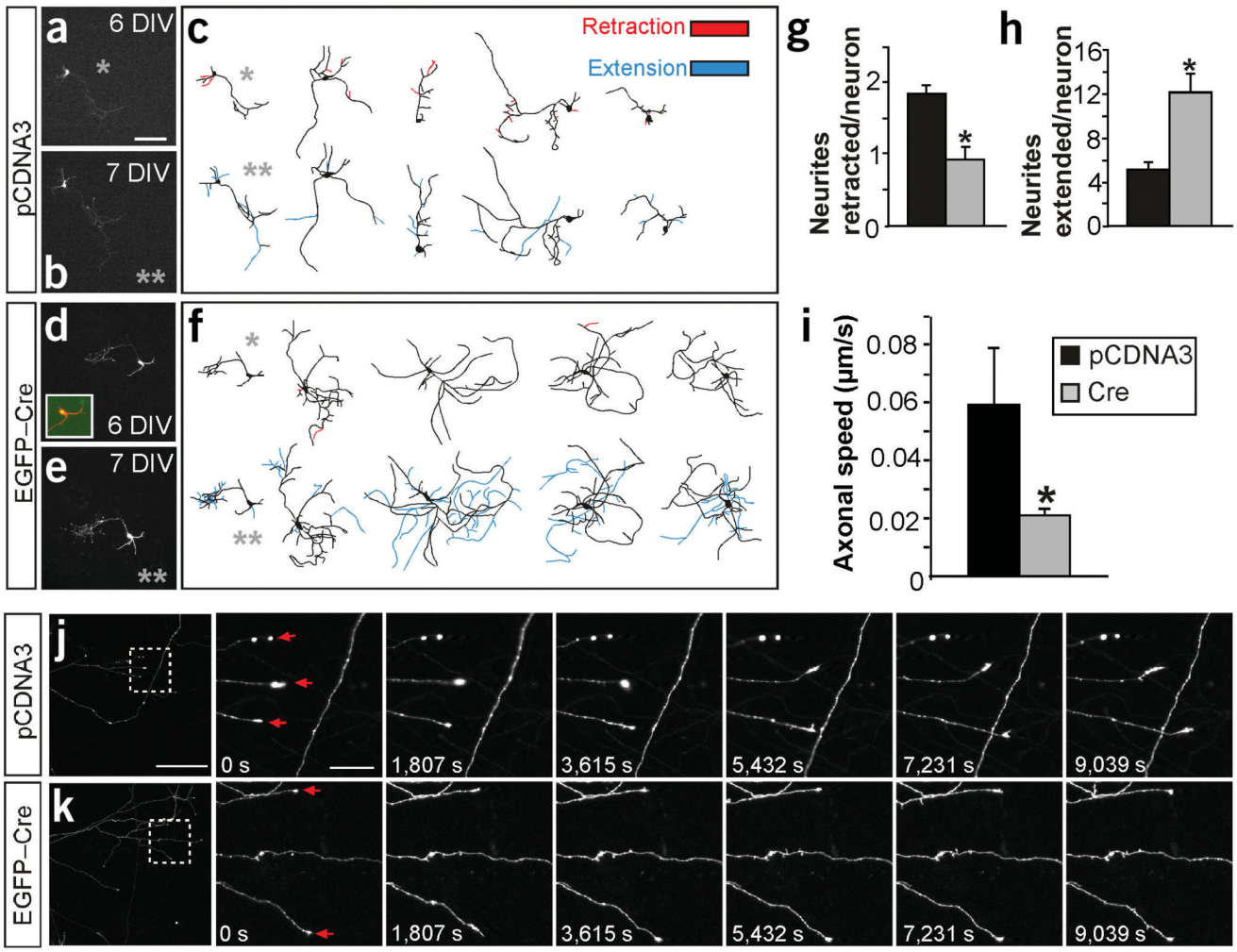

Figure 5.

Axonal branch dynamics of hippocampal neurons in absence of FAK. (**a–h**) Time course recording of the same neuron at 6 and 7 DIV. (**a,c,d,f**) *In vitro* fluorescence images and representative drawings of neurons transfected with control pCDNA3 (**a,c**) or EGFP-Cre (**d, f**) plasmids at 6 DIV. (**b,c,e,f**) Images of the same neurons after 1 d (7 DIV). Inset in **d** shows colocalization of DsRed (red) and EGFP-Cre (green). Gray asterisks identify the drawing of the neurons shown in the adjacent photomicrographs. Neurites undergoing retraction at 7 DIV are shown in red in the 6-DIV drawings. The new extended neurites at 7 DIV are shown in blue in the 7-DIV drawings. (**g**) Quantification of the number of neurites retracted per neuron in the time course experiments. **P* < 0.03 versus control by two-tailed *t*-test (control, 1.86 ± 0.11; mutant, 0.92 ± 0.18). (**h**) Quantification of the neurites extended per neuron in the time course experiments. **P* < 0.001 versus control (control, 5.07 ± 0.74; mutant, 12.07 ± 1.7; *n* = 30 neurons from three independent experiments in **g** and **h**). (**i**) Quantification of the growth cone advance rate expressed in µm progressed per s. **P* < 0.04 versus control (control, 0.05 ± 0.019; mutant 0.02 ± 0.002; *n* = 93 axons from control neurons and 125 axons from Cre-transfected neurons from two independent experiments). (**j,k**) *In vivo* time-lapse imaging of the same axonal branch recorded over 3 h at 15-min intervals. Left image, low-magnification of axonal branches from the pCDNA3 and DsRed (**j**) and the EGFP-Cre and DsRed (**k**) cotransfected neurons. Right images, boxed areas in **j** and **k** shown as higher magnification

time-lapse sequences. Note that, as in Figure 4, most branching neurites at these stages are developing axons (~95%), although a few of them could be dendrites. Data are the mean ± s.e.m. Scale bars, 150 μm (**a–f** and **j,k**, left image); 25 μm (**j, k**, right images).

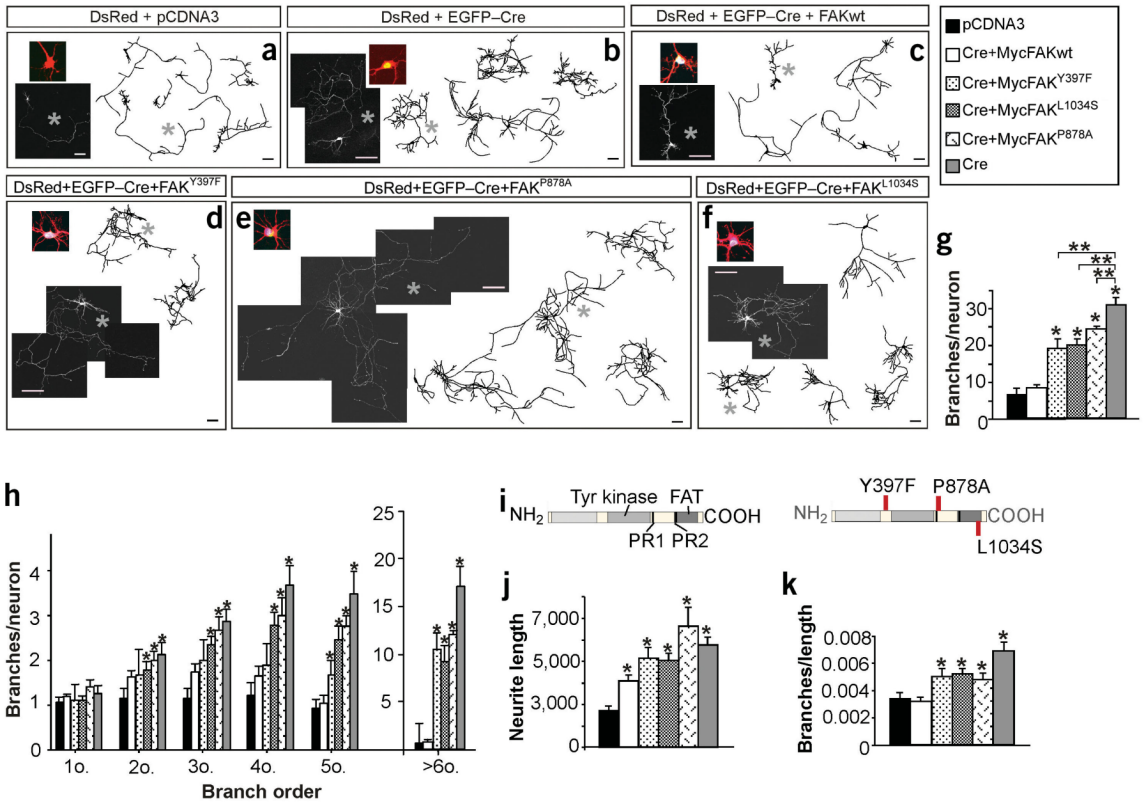

Figure 6.

Several protein-binding sites on FAK are required to control axonal branching as assessed by coexpression experiments with EGFP-Cre. (**a–c**) FAK re-expression reverses *Cre*-mediated *fak* deletion phenotype into a wild-type pattern in mice hippocampal neurons. Fluorescence images and drawings of neurons transfected with pCDNA3, EGFP-Cre and EGFP-Cre plus wild-type FAK. (**d–f**) Fluorescence images and representative drawings taken from coexpression experiments of FAK-defective variants and Cre plasmids. (**d**) Myc-FAK^{Y397F} (**e**) Myc-FAK^{878A} (**f**) Myc-FAK^{1034S}. All neurons were transfected at 3 DIV and recorded at 6 DIV. High-magnification images in color show colocalization (yellow or white) of DsRed, EGFP-Cre and Myc. (**g**) Quantification of the total number of branches per neuron. One asterisk denotes significant difference from control; two asterisks denote significant difference from Cre experiments. $P < 0.01–0.0001$ (control, 6.21 ± 1.07; Cre, 30.53 ± 2.07; FAKwt, 8.07 ± 0.68; FAK^{Y397F}, 18.88 ± 2.39; FAKP^{878A}, 23.50 ± 2.80; FAK^{L1034S}, 19.66 ± 1.76; $n = 93$ neurons from three independent experiments in **g**,**h**,**j**,**k**). (**h**) Quantification of the number of increasing branch order per neuron. $P < 0.05$ to $P < 0.0001$ versus control. (**i**) Position of point mutations and protein domains in FAK. FAT, focal adhesion targeting region, PR1 and PR2, proline-rich regions. (**j**) Quantification of the total neurite length per neuron expressed in um. $P < 0.05–0.0001$ versus control (control, 1,705.71 ± 265.34; Cre, 4,748.76 ± 402.85; FAKwt (3,061.96 ± 335.56; FAK^{Y397F}, 4,120.26 ± 543.10; FAK^{P878A}, 6279.38 ± 922.08; FAK^{L1034S}, 4,018.83 ± 347.92). (**k**) Quantification of the total number of branches per µm of neurite. $P < 0.05–0.0001$ versus control (control, 0.0034 ± 0.0004; Cre, 0.0068 ± 0.0006; FAKwt, 0.0032 ± 0.0003; FAK^{Y397F}, 0.005 ± 0.0005; FAK^{P878A}, 0.0045 ± 0.0005; FAK^{L1034S}, 0.0052 ± 0.0004) Note that ectopic expression of FAK rescues both the branching and the overall increase in axon length phenotypes in FAK-deficient neurons. This result is consistent with our observations that loss of FAK resulted in reduced axonal growth speed, and supports the idea that FAK controls axonal dynamics by participating both in axonal growth

and branch formation independently. Note that, as shown in Figure 4, most branching neurites at these stages are developing axons (~95%), although a minor percentage of them could be dendrites. Data are the mean ± s.e.m. Scale bars, 200 μm (**a–g**).

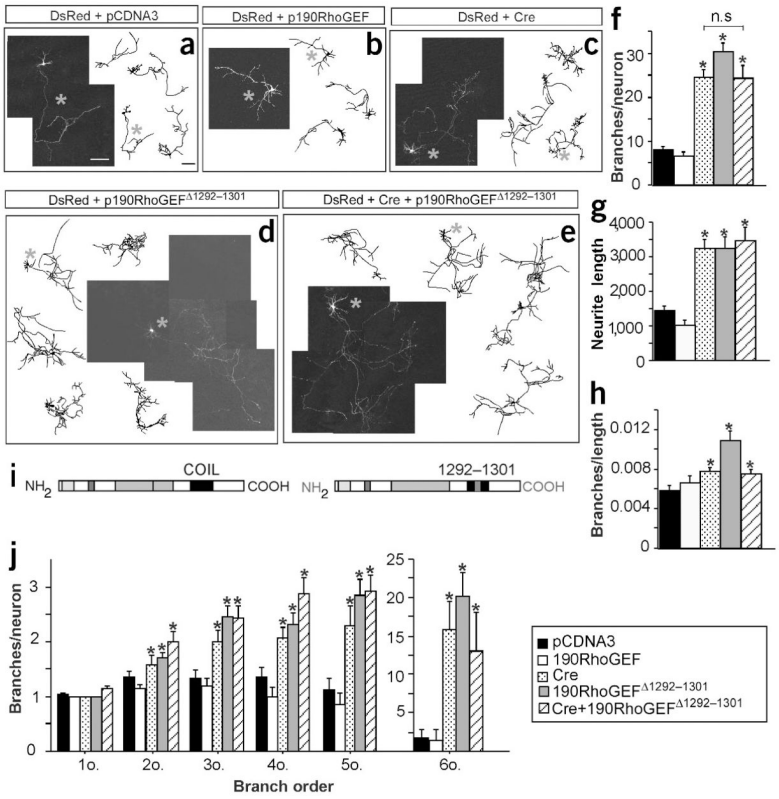

Figure 7.

The structural integrity of residues 1,292–1,301 in p190RhoGEF is required to control axonal branching. (**a–e**) Fluorescence images and representative drawings at 6 DIV of neurons that were transfected at 3 DIV with control pCDNA3 (**a**), full-length p190RhoGEF (**b**), Cre (**c**), p190RhoGEF$^{\Delta1292–1301}$ (**d**), and Cre plus p190RhoGEF$^{\Delta1292–1301}$ (**e**). (**f**) Quantification of the total number of branches per neuron. *P < 0.0001 versus control by ANOVA (pCDNA3, 7.92 ± 0.81; p190RhoGEF, 6.61 ± 0.98; Cre, 24.64 ± 1.60; p190RhoGEF$^{\Delta1292–1301}$, 30.45 ± 1.98; Cre plus p190RhoGEF$^{\Delta1292–1301}$, 24.39 ± 2.71; n = 122 neurons from 3–5 independent experiments in **f–h,j**). n.s., not significant. (**g**) Quantification of the total neurite length per neuron expressed in μm.*P < 0.0001 versus control (pCDNA3, 1,439.02 ± 132.817; p190RhoGEF, 1,034.74 ± 118.60; Cre, 3,253.46 ± 243.30; p190RhoGEF$^{\Delta1292–1301}$; 3,254.06 ± 341.44; Cre plus p190RhoGEF$^{\Delta1292–1301}$, 3,482.34 ± 375.67). (**h**) Quantification of the total number of branches per μm of neurite. *P < 0.05–0.0001 versus control (pCDNA3, 0.0058 ± 0.0005; p190RhoGEF, 0.0066 ± 0.0028; Cre, 0.0077 ± 0.0004; p190RhoGEF$^{\Delta1292–1301}$, 0.0108 ± 0.001; Cre plus p190RhoGEF$^{\Delta1292–1301}$, 0.0074 ± 0.0005). (**i**) Full-length p190RhoGEF, showing the region truncated. (**j**) Quantification of branches at ncreasing branch orders per neuron. Note that, as shown in Figure 4, most branching neurites at these stages are developing axons (~95%), although a few could be dendrites. *P< 0.0001. Data are mean ± s.e.m. Scale bars, 200 μm (**a–c**).